Long-period (3 to 16 s) Ground Motions in and around the Los Angeles Basin during the Mw 7.2 El Mayor-Cucapah Earthquake of April 4, 2010

K. Hatayama
National Research Institute of Fire and Disaster (Japan)

E. Kalkan
U.S. Geological Survey

SUMMARY:
We evaluated spectral amplification factors of long-period ground motions (3 to 10 s) in the Los Angeles (LA) basin with respect to its surrounding reference hard-rock sites from the Mw7.2 April 4, 2010 El Mayor-Cucapah earthquake records and presented period-specific maps of amplification factors for long periods. This earthquake was the first event providing many (236) high-quality recordings to study spatial variation of long-period amplification in the LA basin. We also tried numerical wave propagation simulations for one of the recent 3D seismic-velocity models for south California: CVM-H 6.2. From comparison of the observed amplification factors with the simulated ones, the CVM-H 6.2 is considered to be almost enable to account for the observed amplification factors with periods from 8 to 10 s in the LA basin, and it leaves more to be improved so that the observed shorter-period (4 to 6 s) amplification factors can be better simulated.

Keywords: Long-period ground motion, Los Angeles Basin, El Mayor-Cucapah earthquake of Apri 4, 2010

1. INTRODUCTION

The Mw7.2 El Mayor-Cucupah earthquake that occurred in northern Baja California on April 4, 2010 was the first event not only shaking southern California with a magnitude over 7 since the 1999 M_L7.1 Hector Mine earthquake, but also providing the largest number of recordings with long-period (3 to 10 s) content in the region. Graves and Aagaard (2011) used the ground motion data set of this event to test long-period ground motion simulations of scenario earthquakes. Using the same data set, we examined here the long-period ground motion amplification in the Los Angeles (LA) basin. The amplification of long-period ground motions could be critical for structures having long vibration periods; these structures are high-rise buildings, base-isolated buildings, long-span bridges and large-diameter oil tanks. In the LA basin, high-rise buildings are concentrated in downtown LA and Century City, and large-diameter oil tanks are clustered near Manhattan Beach in the western part of the basin and in Long Beach. During the Mw8.0 2003 Tokachi-oki, Japan earthquake, the long-period strong ground motions excited the liquid sloshing in large-diameter oil tanks, and caused severe damage, including tank fire and sinking of the floating roof, to many of them (Hatayama et al., 2007; Hatayama, 2008).

In the sections that follow, we first describe the distribution of the long-period PGV values observed in southern California during the El Mayor-Cucapah earthquake to provide an overview of the observed long-period ground motions. We then show the spectral amplification factors of long-period ground motions in and around the LA basin with respect to selected hard-rock reference sites. Finally, the observed spectral amplification factors are tried to simulate by using a 3D seismic-velocity model for southern California: the Southern California Earthquake Center Community Velocity Model (CVM-H 6.2; http://structure.harvard.edu/cvm-h/) to show how it can account for the observation.

2. OBSERVED GROUND VELOCITY

Most of the ground motions used in this study are obtained from the Center for Engineering Strong Motion Data (http://www.strongmotioncenter.org/). Records having a duration less than 60 s were not used, because they are unlikely to contain enough long-period content. Fig. 2.1 shows the location of a total of 359 stations that recorded this event; the epicentral distance of these stations ranges from 20 to 400 km.

Figure 2.2 shows the PGV contours computed from the time series of the root mean squares of the two horizontal components of processed velocity records. These records were processed by bandpass filtering with a passing period range of 3 to 16 s. In the LA basin, higher PGV values with long periods, observed relative to its surrounding area, indicate strong amplification of long-period ground motions. Although, the LA basin is about 300 km away from the source, the PGV values were as high as at those stations located 150 km away from the epicenter. Also shown in Fig. 2.2 are the higher PGV values observed in the San Bernardino valley. A detailed map of the PGV contours in and around the LA basin is shown next in Fig. 2.3, which denotes the highest long-period PGV values (0.12 m/s) in the central part of the LA basin (around Downey) and the western part of the basin (around Manhattan Beach). Near Manhattan Beach, there are many large floating roof oil tanks with natural periods at several seconds. Relatively higher PGV values (~ 0.08 m/s) were also observed in the San Gabriel (SG) valley (around Baldwin Park).

In order to examine the wave propagation within the LA basin, the N303°E- and N213°E-component velocity waveforms processed by bandpass filtering with a passing period range of 3 to 16 s are plotted in Fig. 2.4, where the N303°E and N213°E correspond to the radial and transverse directions, respectively, with respect to the one from the source to the basin. Fig. 2.4 (c) identifies the location of corresponding stations along the line passing from the source to the central part of the basin. It is evident that the velocity wave train carrying the PGV values developed significantly with the growth of amplitudes and the elongation of duration as it propagated from the source-side edge (station STG) into the basin. The amplitudes of the wave train reached to a maximum around the central part of the basin (stations 14368 and 14175), and decreased after the wave train passed this location. This figure clearly demonstrates the evolution of long-period ground motions within the LA basin.

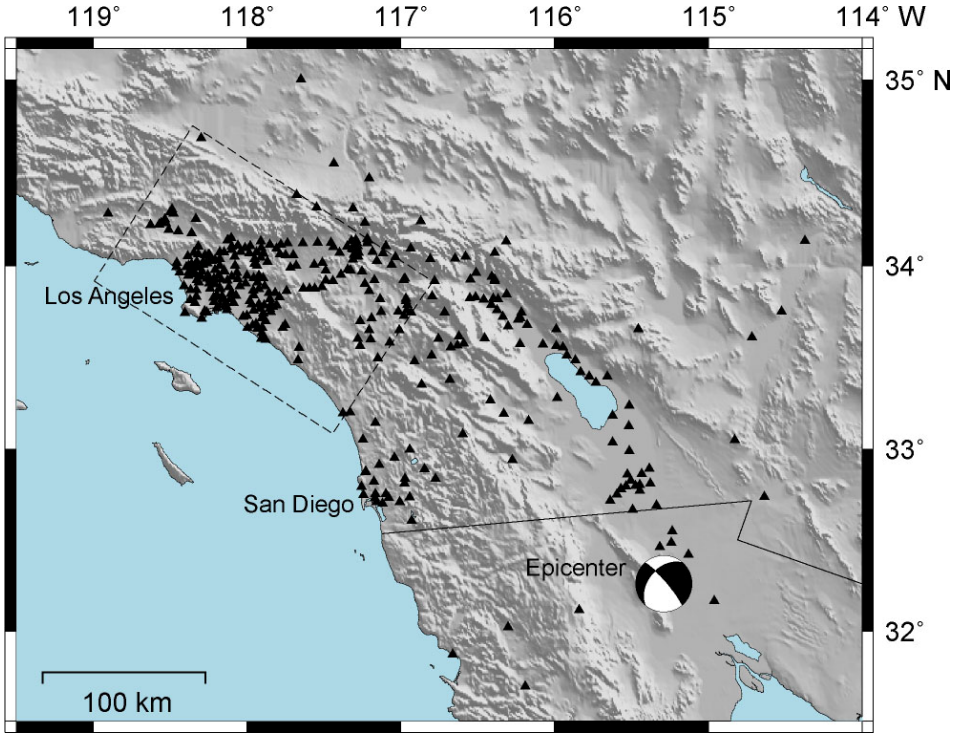

Figure 2.1. Strong ground motion stations whose records were used in this study (triangles)

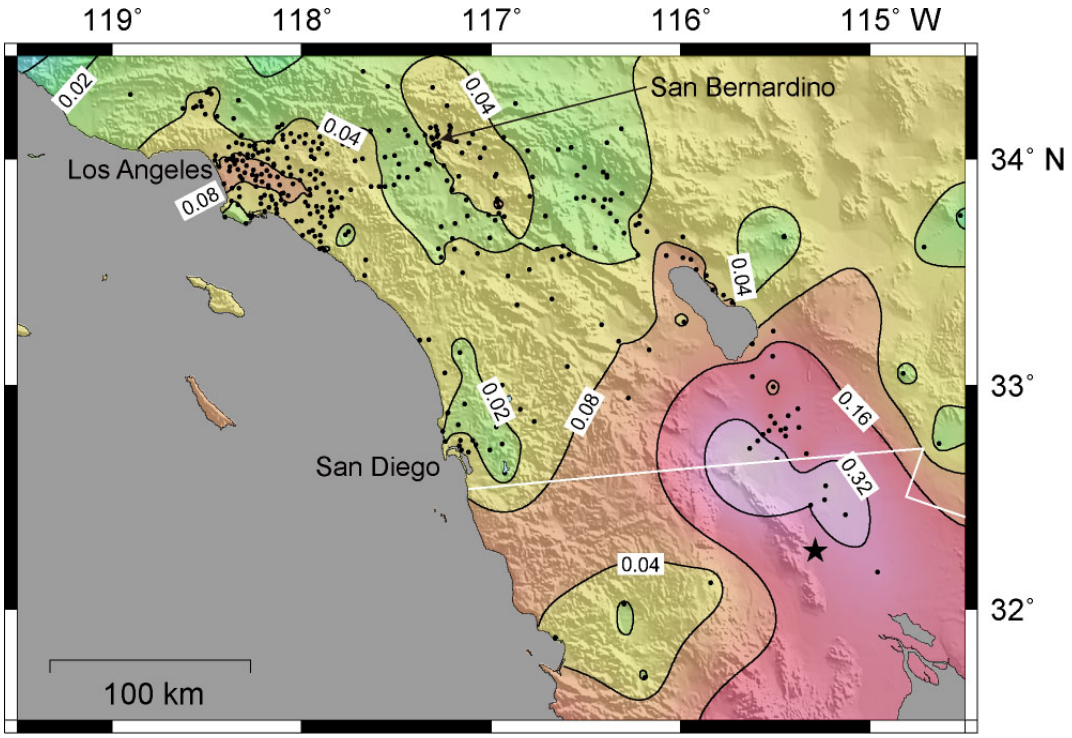

Figure 2.2. Observed PGV values (m/s) with a period range of 3 to 16 s observed in southern California

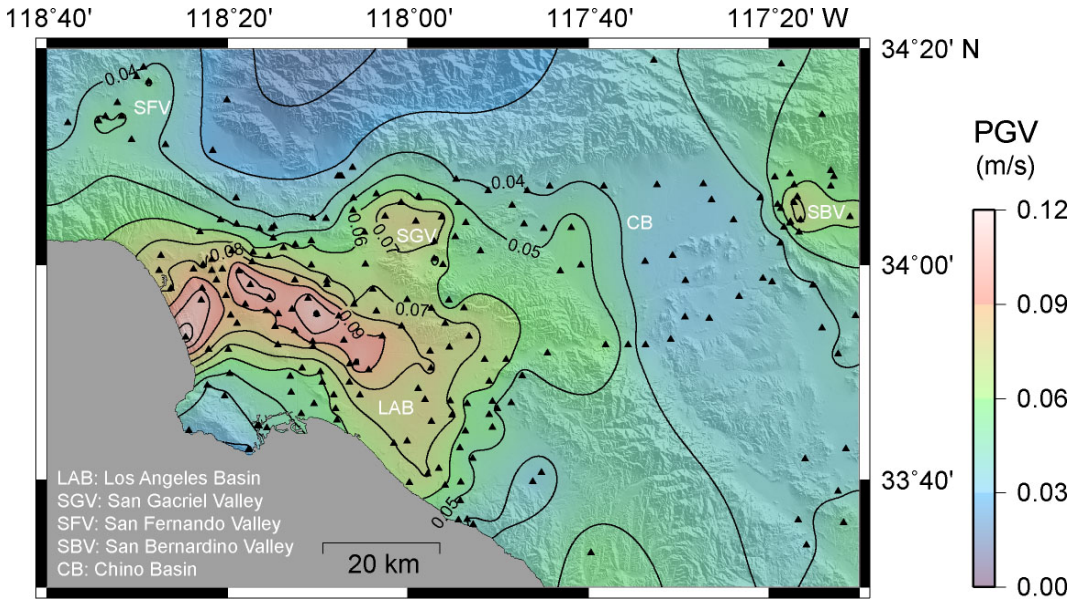

Figure 2.3. Observed PGV values (m/s) with a period range of 3 to 16 s in and around the Los Angeles (LA) basin

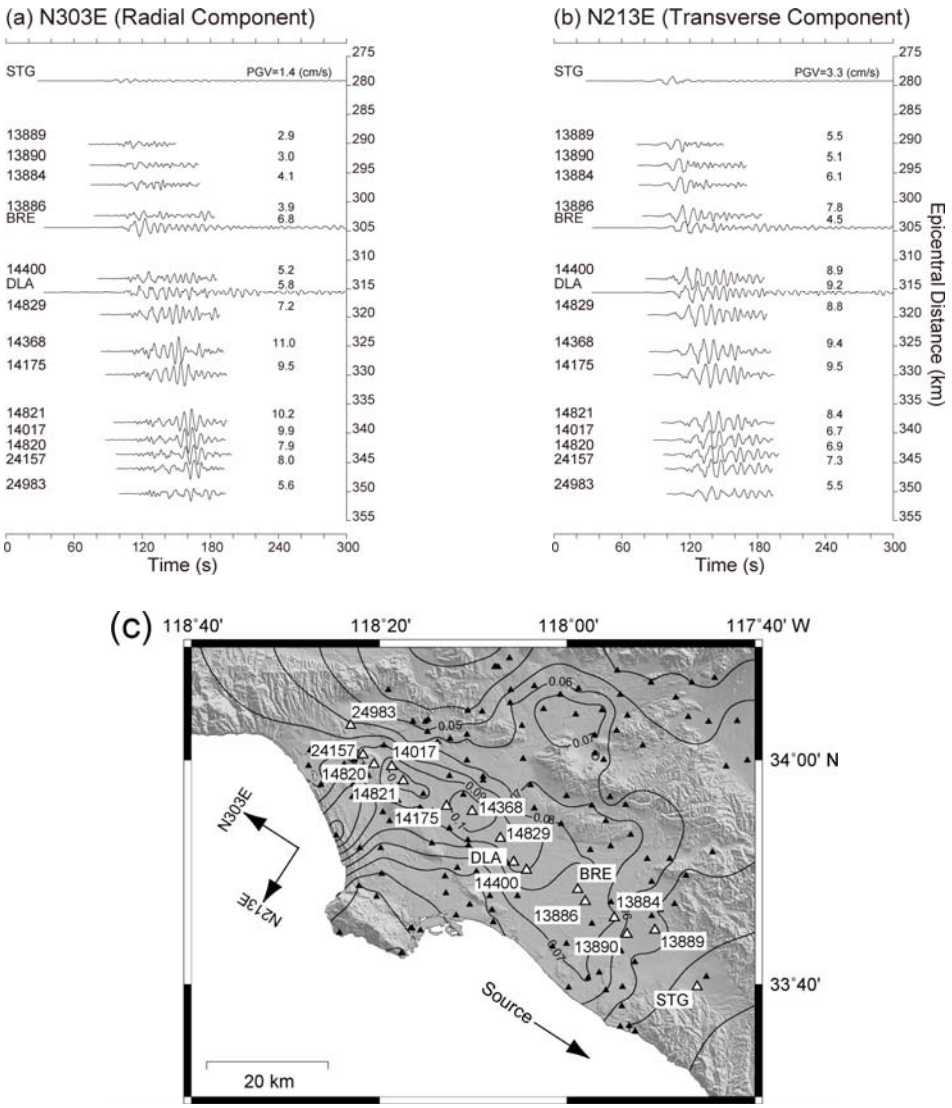

Figure 2.4. Observed velocity waveforms with a period range of 3 to 16 s in the LA basin

3. OBSERVED AMPLIFICATION FACTORS OF FOURIER SPECTRA

We evaluated the spectral amplification factors of long-period ground motions for the LA basin with respect to the surrounding hard-rock reference sites, by using the El Mayor-Cucapah earthquake data from 236 stations falling into the area denoted by the broken lines in Fig. 2.1.

Fig. 3.1 shows the Fourier acceleration spectra from those 236 stations (the gray and orange lines). The spectral ordinates plotted are the geometric mean of the two-horizontal-component spectra. At periods over 3 s, a group of spectral peaks between 5 and 9 s is evident, indicating that a number of recordings in and around the basin has dominant long-period components. The maximum peak, reaching 0.12 m/s at the station 14221 (Manhattan Beach), has the highest PGV value.

The spectral amplification factors were evaluated by computing spectral ratios of the Fourier acceleration spectra shown in Fig. 3.1 at each station with respect to reference stations on hard-rock surrounding the LA basin. The reference stations were selected according to the following three criteria: (1) the record length should be long enough; (2) the basin underground seismic-velocity model does not suggest that the station is located on sediments; (3) the observed spectral accelerations should be relatively small. Regarding criterion (1), we selected the stations with a record length longer than 300 s. Fig. 3.2 shows the stations following criterion (1) by white triangles. To apply criterion (2),

we calculated the surface-wave phase velocities by using the CVM-H 6.2, and then selected those stations from the sites where the surface-wave phase velocities are high enough that they cannot be considered to be located on sediments. The colors in Fig. 3.2 show the phase velocities of the fundamental-mode Love waves at a period of 4 s. Because the CVM-H 6.2 is a continuous model, where the material parameters such as S-wave velocities vary continuously in both lateral and vertical directions, we assumed a 1-D layer-wise velocity model based on the CVM-H 6.2 for each site where the surface wave phase velocities were calculated. We supposed that the contour line of the phase velocity of around 2.2 km/s indicate the boundary between the sediment sites and the rock sites in this model, and we selected the stations from those sites where the phase velocity is mostly over 2.2 km/s. Applying criterion (3), we finally identified 17 reference stations denoted by the squares in Fig. 4.2.

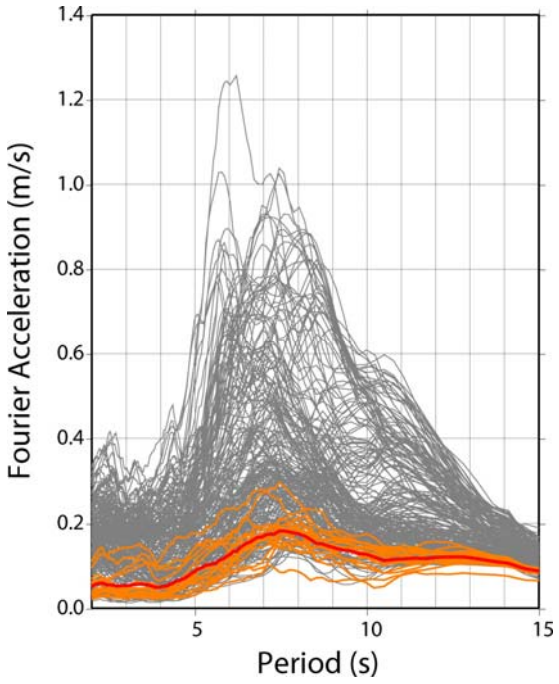

Figure 3.1. Observed Fourier acceleration spectra from the stations located in and around the LA basin

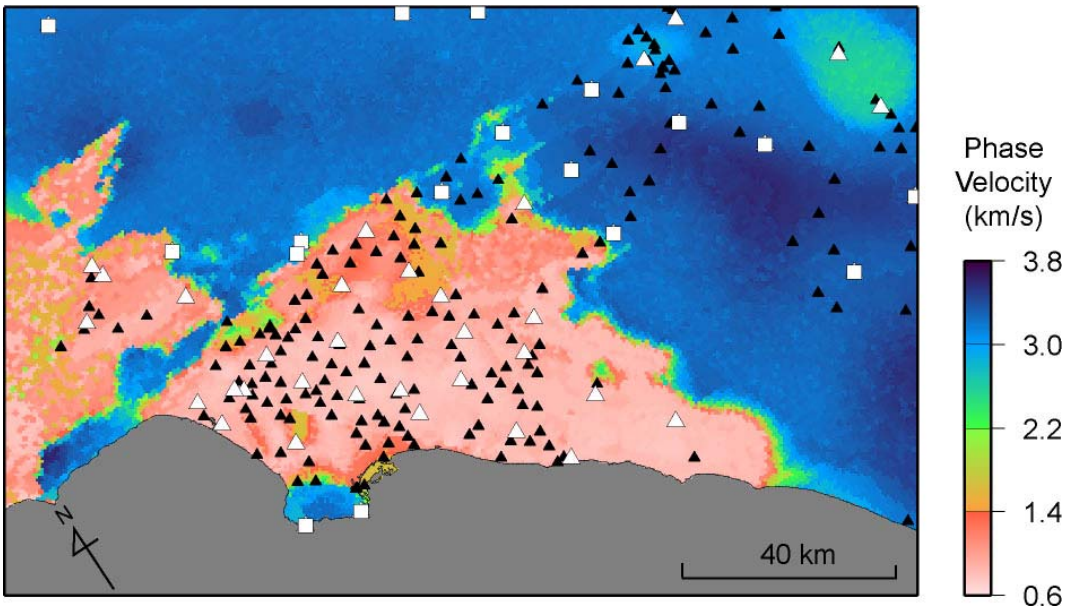

Figure 3.2. Phase velocity of the fundamental-mode Love waves at a period of 4 s

The orange lines in Fig. 3.1 represent the spectral ordinates from those 17 reference stations, and the red line shows their arithmetic mean. We divided the Fourier spectra of all the stations by the arithmetic mean, and then obtained the amplification factors with respect to the reference hard-rock sites as shown in Fig. 3.3. In the period range between 3 and 11 s, large amplification factors over 5 are observed at a number of stations, and high peaks appear at periods of 4 and 6 s. The maximum amplification factor exceeding 10 is observed at station 14221 (close to Manhattan Beach), where the highest Fourier acceleration spectral ordinate was observed (cf. Fig. 3.1). The amplification factors decrease beyond 11 s.

Fig. 3.4 shows the maps of the observed spectral amplification factors at 10 (O-a), 8 (O-b), 6 (O-c) and 4 s (O-d). In these maps, the spectral amplification factors calculated for each station, shown in Fig. 3.3, are interpolated geometrically without considering the underground seismic-velocity structure. For a period of 10 s, the largest amplification factor of about 5 occurs in the central part of the LA basin. For 8 s, larger amplification factors are evident in the SG valley and the central part of the LA basin. For 6 s, the largest amplification is observed in the western part of the basin (Manhattan Beach), although the amplification in the central part is also large. Around Manhattan Beach, the ground motions with this period are amplified by a factor of 10. For 4 s, the largest amplification factor of about 8 occurs in the central part of the LA basin.

In the SG valley, large amplification does not occur for a period of 10 s, but does for periods of 8, 6 and 4 s. In the central part of the LA basin, however, large amplification is observed for all these periods. This implies that the sediments in the SG valley are not as soft and/or thick as the ones in the central part of the LA basin. Looking at the south-eastern part of the LA basin, large amplification occurs only for 4 s, indicating that the sediments in the south-eastern part of the LA basin are thinner and/or harder than the ones in the central part of the LA basin.

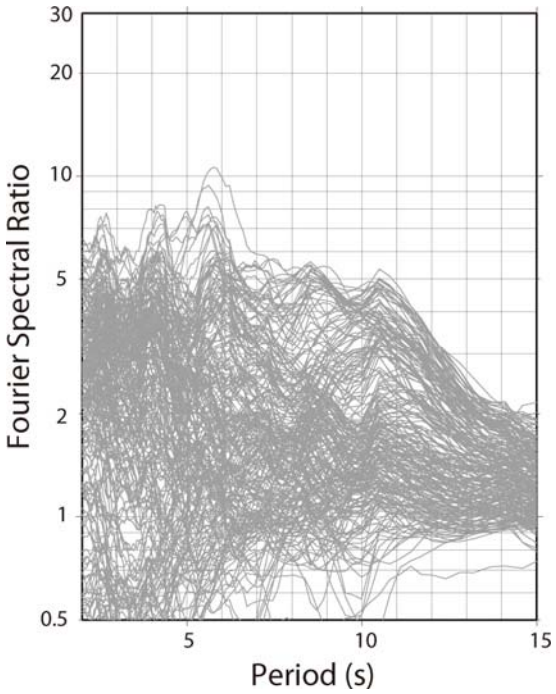

Figure 3.3. Observed spectral Amplification factors in and around the LA basin

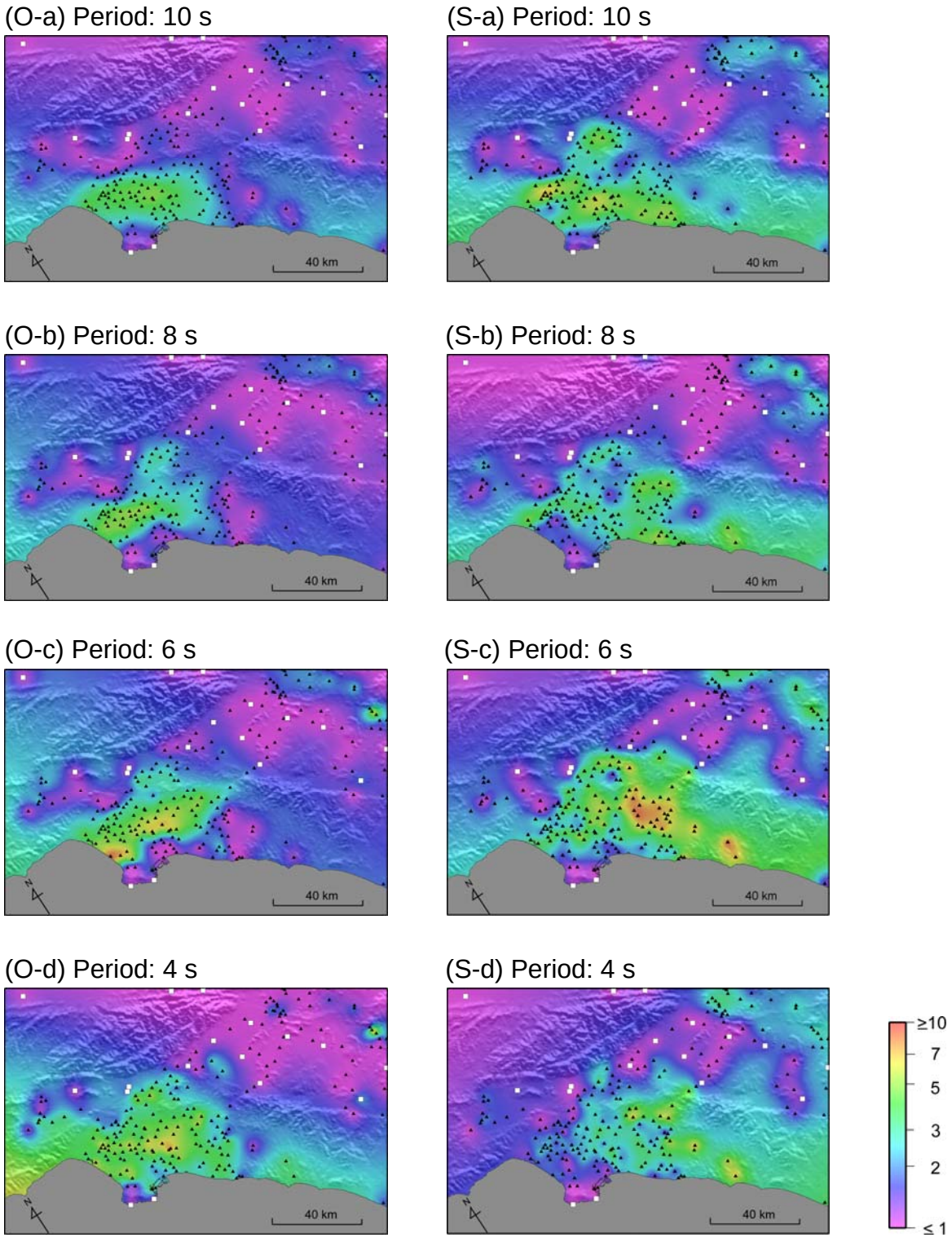

Figure 3.4. Period-specific amplification factors in and around the LA basin

4. NUMERICAL SIMULATION OF SPECTRAL AMPLIFICATION FACTORS

In order to investigate how the observed spectral amplification factors for the long-period ground motions shown in the previous section can be accounted for by the present knowledge on underground structure of the LA basin, we tried 3D numerical wave propagation simulations for one of the recent 3D seismic-velocity models for south California: CVM-H 6.2.

The finite-difference-method (FDM) -based technique proposed by Zahradník and Moczo (1996) was used to simulate velocity waveforms within the area denoted by the broken lines in Fig. 2.1, where the LA basin is encompassed and the 3D seismic-velocity structure was assumed based on the CVM-H 6.2. In the technique that we used, the inner area of the broken lines was modelled by FDM with velocity-stress staggered grids for velocity waveforms to be calculated, while the outer area of the broken lines was assumed horizontally layered media, because it could be considered relatively harder and simpler than the one within the LA basin, and the velocity waveforms in that area were calculated by a discrete wave-number summation method. The horizontally layered media for the outer area was assumed again based on the CVM-H 6.2. The continuous boundary conditions in the seismic wave-field between the inner and the outer areas were imposed in calculating the wave-field within an array of grids that is located in the margins of the inner area bordering the outer area. This marginal array plays the same role of "source box" that was proposed by Alterman and Karal (1968), transmitting incident waves from the outer area into the inner area as well as scattered waves from the inner are, which includes irregularity, to the outer area. It was because of two reasons why we used the above technique instead of the ordinary FDM. One was a positive reason that we would like to simulate simple basin amplification effects rather than combined effects due to both the basin and the path from the source to the basin. For this sake, we did not include the effects from realistic and somewhat complex underground structures in the path, but assumed a simple underground structure in the path. The other was a negative reason: limitation of computational resources. The technique that we used does not demand discretizing a vast area encompassing both the far source and the LA basin at the same time.

We assumed a double-couple point source with the same focal mechanism as the El Mayor-Cucapah earthquake at its hypocentral location. The impulse responses from the point source were computed at each of the source box grids at first and then those impulse responses were convolved with an observation-based transfer function to obtain velocity waveforms in which the source time function was taken into account. The convolution was computed in the frequency domain, the transfer function being assumed to be the spectral ratio of the ground motions recorded at one of the stations during the El Mayor-Cucapah earthquake with respect to the impulse responses computed for the same station. The station where the spectral ratio was computed for the observation-based transfer function was one that was located between the source and the LA basin and close to the border of the inner and the outer areas.

The acccuracy of the finite difference approximation for the inner area was the 2nd- and the 4th-order, respectively. The horizontal and the vertical grid intervals were 0.3 and 0.2 km, respectively, and the S-wave velocities less than 0.5 km/s in the CVM-H 6.2 were rounded up to 0.5 km/s in our modeling, allowing an available period range over 3 s for the simulated ground velocities. The Q-values were assumed based on Olsen et al. (2003).

The amplifications factors for the simulated long-period ground motions were evaluated by the same manner as those for the observed ones using the simulated ground velocities. The results are shown in Fig. 3.4 (S-a) to (S-d), compared with the observed amplifications factors (O-a) to (O-d). For a period of 10 s, the simulated amplification factors well agree with the observed ones in the central and western part of the LA basin. The simulation also indicates the large amplification even in the SG valley and the south-eastern part of the LA basin, which disagrees with the observation. For 8 s, not only the central part of the LA basin but also the SG valley is well simulated in terms of good agreements between the observed and the simulated amplification factors. The observed large amplification in the western part of the LA basin however is failed to simulate. In the south-eastern part of the LA basin, the non-observed large amplification is again simulated. For 6 s, there is significant discrepancy between the observation and the simulation in terms of the places where the largest amplification occurs: the largest amplification was observed in the western part of the basin (Manhattan Beach), while it was simulated in the eastern part and the south-eastern part of the LA basin. Good agreements in the SG valley are again observed. For 4 s, the simulated large amplification in the south-eastern part of the LA basin agrees with the observed one, but the amplification pattern in the other areas is failed to simulate. The CVM-H 6.2 is considered to be almost enable to account for

the observed amplification factors with a period range of 8 to 10 s in the LA basin, and it leaves more to be improved so that the shorter-period (4 to 6 s) amplification factors can be better simulated.

6. CONCLUSIONS

The Mw7.2 El Mayor-Cucapah earthquake of April 4, 2010 was recorded at 236 strong ground motion stations in and around the Los Angeles (LA) basin that is about 300 km away from the source. This earthquake is the largest event providing a large number of high-quality recordings to study spatial variation of long-period ground motion amplification in and around the LA basin. The PGV in the basin reached to 0.12 m/s within a period range of 3 to 16 s. The ground motions in and around the basin were dominated by long-period components; their Fourier acceleration spectra have a peak around 6 s. The velocity waveforms recorded in and around the LA basin clearly demonstrates evolution of the long-period ground motions within the LA basin.

In this paper, we evaluated spectral amplification factors of long-period ground motions in and around the LA basin with respect to the 17 reference hard-rock sites surrounding the basin from the El Mayor-Cucapah earthquake records and presented period-specific maps of amplification factors for periods of 10, 8, 6 and 4 s. We also tried 3D numerical wave propagation simulations for one of the recent 3D seismic-velocity models for south California: CVM-H 6.2 in order to investigate how the observed long-period spectral amplification factors can be accounted for by the present knowledge on underground structure of the LA basin.

From comparison of the period-specific maps of amplification factors between the observation and the simulation, the CVM-H 6.2 is considered to be almost enable to account for the observed amplification factors with a period range of 8 to 10 s in the LA basin, and it leaves more to be improved so that the observed shorter-period (4 to 6 s) amplification factors can be better simulated.

For a period of 10 s, the largest amplification factor of about 5 occurs in the central part of the LA basin, which is well simulated in terms of good agreements between the observed and the simulated amplification factors. The simulation also indicates the large amplification even in the San Gabriel (SG) valley and the south-eastern part of the LA basin, which disagrees with the observation.

For 8 s, larger amplification factors are evident in the SG valley and the central part of the LA basin, which are also well simulated. In the south-eastern part of the LA basin, the non-observed large amplification is again simulated. The simulation disagrees with the observation even in the western part of the LA basin: the simulation undershoots the observation.

For 6 s, the largest amplification is observed in the western part of the basin (Manhattan Beach), although the amplification in the central part is also large. Around Manhattan Beach, the ground motions with this period are amplified by a factor of 10. There is significant discrepancy between the observation and the simulation in terms of the places where the largest amplification occurs: the simulation indicates the largest amplification in the eastern part and the south-eastern part of the LA basin.

For a period of 4 s, the largest amplification factor of about 8 occurs in the central part of the LA basin. Large amplification was also observed in the eastern part and the south-eastern part of the LA basin, where for the other three periods large amplification was not seen. Although the simulated large amplification in the south-eastern part of the LA basin agrees with the observed one, the amplification pattern in the other areas is failed to simulate.

AKCNOWLEDGEMENT
Ken Hatayama would like to acknowledge the generous support of the Excellent Young Researchers Overseas Visit Program of Japan Society for the Promotion of Science for providing him the financial support for this investigation. We wish to thank Brad Aagaard and Robert Graves for their reviews of this article.

REFERENCES

Alterman, Z. and Karal, F.C.Jr. (1968). Propagation of elastic waves in layered media by finite difference methods, *Bull. Seism. Soc. Am.* **58**, 367-398.

Graves, R.W. and Aagaard, B.T. (2011). Testing long-period ground-motion simulations of scenario earthquakes using the Mw 7.2 El Mayor-Cucapah mainshock: evaluation of finite-fault rupture characterization and 3D seismic velocity models. *Bull. Seism. Soc. Am.* **101:2**, 895-907.

Hatayama, K. (2008). Lessons from the 2003 Tokachi-oki, Japan, earthquake for prediction of long-period strong Ground motions and sloshing damage to oil storage tanks. *J. Seismol.* **12**, 255-263.

Hatayama, K., Kanno, T. and Kudo, K. (2007). Control factors of spatial variation of long-period strong ground motions in the Yufutsu sedimentary basin, Hokkaido, during the Mw 8.0 2003 Tokachi-oki, Japan, earthquake. *Bull. Seism. Soc. Am.* **97:4**, 1308-1323.

Olsen, K.B., Day, S.M. and Bradley, C.R. (2003). Estimation of Q for long-Period (>2 sec) waves in the Los Angeles basin. *Bull. Seism. Soc. Am.* **93:2**, 627-638.

Zahradník, J. and Moczo, P. (1996). Hybrid seismic modeling based on discrete-wave number and finite-difference methods, *PAGEOPH* **148**, 21-38.